

Magnetic and superconducting properties of Fe/Nb multilayered films

K. Kawaguchi and M. Sohma

National Chemical Laboratory for Industry, 1-1 Higashi, Tsukuba, Ibaraki 305, Japan

(Received 2 March 1992)

We have prepared ferromagnetic (Fe) and superconducting (Nb) multilayered films, whose structural properties depend on the choice of substrate. The magnetic properties were investigated by use of magnetization and hyperfine field measurements. The multilayered films with Fe layers thinner than 3.0 do not exhibit spontaneous ferromagnetic ordering. Their superconducting behavior changes from two dimensional to three dimensional as the Fe-layer thickness decreases. The critical thicknesses at which the superconductive dimensionality changes and at which the ferromagnetism disappears do not coincide. Some samples with monatomic Fe layers showed an anomalous anisotropy in the upper critical field (H_{c2}).

I. INTRODUCTION

It is well known that ferromagnetic ordering and superconducting electron Cooper pairing cannot coexist within the framework of BCS theory. Studies of certain rare-earth element compounds, however, indicated that such coexistence was possible.¹ In these cases, $4f$ electrons which contribute to the magnetic moment are localized; consequently the interaction between superconductivity and ferromagnetism is considered to be fairly weak. On the other hand, $3d$ electrons which govern the magnetic properties of transition-metal ferromagnetic elements will interact strongly with the superconductivity. We expect to gain fruitful information on both magnetism and superconductivity by studying this interaction. This appears to be a difficult task for bulk materials, because the presence of a small amount of $3d$ ferromagnetic impurities suffices to destroy superconductivity. The multilayering technique considered is a promising technique for this study, because it separates two materials chemically and can, therefore, make conditions favorable for such interactions. Furthermore, this technique makes it possible to control the magnetic behavior to a certain extent by varying the magnetic-layer thickness.

There have been some noteworthy reports relating to the aforementioned subject. Fe/Pb multilayers have been prepared and both tunneling and resistance measurements were performed *in situ*.² The results indicated that only one or two atomic Fe layers could destroy the interlayer superconductive coherence. In a study of the V/Fe system,³ on the contrary, both a 2D-3D crossover and a ferromagnetism have been observed on the same sample. It implies the coexistence of both superconducting and ferromagnetic electrons in the Fe layers. A somewhat different result has been reported in a study of the Ni/V system.⁴ The superconducting behavior strongly depends on the magnetic properties of Ni layers. Ni layers thicker than 1.0 nm are found to be ferromagnetic and decouple the interlayer superconductive coherence. Conversely, thinner Ni layers for which ferromagnetism disappeared could not break the coherence strongly enough and therefore showed an anomalous behavior in upper critical

fields (H_{c2}). The anisotropy of the upper critical fields which are directed parallel [$H_{c2\parallel}(T)$] and perpendicular [$H_{c2\perp}(T)$] to the film plane is reversed near the superconducting transition temperature (T_c). It reverted to normal behavior in the low-temperature region far from T_c . This behavior has been explained semiquantitatively by considering the anisotropic paramagnetic susceptibility as a pair-breaking factor.⁵ These three studies showed three different results; however, detailed information on magnetic properties is still lacking.

In this work, we present not only superconducting properties but also detailed magnetic properties of the Fe/Nb system. Since the T_c of multilayers is usually lower than that of bulk due to the proximity effect, the use of the highest- T_c element (Nb with $T_c=9.3$ K) is desirable. Iron was chosen as a ferromagnetic transition-metal element, because fruitful information on the hyperfine field could be extracted by use of Mössbauer spectroscopy.

II. SAMPLE PREPARATION

The samples were prepared by use of an ultrahigh-vacuum (UHV) deposition method. Refractory metals such as Nb, Ta, and W are generally deposited by a sputtering method. In most popular way to produce multilayered samples by sputtering, the substrate is rotated above two sputtering guns.⁶ This is an effective method for samples composed of alternate layers with nearly the same thickness. In this work, however, our interest lies instead in samples composed of extremely thin ferromagnetic layers and thick superconducting layers. Since thickness ratio is very large, the UHV deposition method is preferable. The deposition chamber was first evacuated to lower than 1×10^{-10} Torr with use of a turbomolecular pump (330 1/s) and a cryopump (10 000 1/s). Each 99.9% purity iron and 99.95% purity niobium ingot used as a source material was heated by each electron beam gun (10 kV acceleration) and evaporated. Both deposition thickness and deposition rate were monitored *in situ* by a quartz-crystal oscillating thickness monitor (QCOTM). Since Nb has a high melting temperature, it

emitted much thermal radiation during deposition, which caused serious inaccuracies for the temperature-sensitive QCOTM. To reduce effects of this thermal radiation, we put the sensor at the substrate far from the source, wrapped it in aluminum foil, and opened a hole to allow the evaporant flux to hit the sensor. Thus, the thickness control of Nb layers was substantially improved. The electron-beam currents of the deposition sources were automatically controlled by the QCOTM and the deposition rates were well regulated. Each pneumatic shutter above the deposition source was opened and closed by a signal from the QCOTM. The multilayering deposition sequence was automatically executed in this way. The UHV was maintained around 1×10^{-9} Torr during the deposition. The substrate was rotated at about 10 rpm to minimize the thickness distribution of the deposited films. The substrate temperature (T_s) dependence was examined at 400 and 200 °C. There were no significant differences among the x-ray diffraction (XRD), magnetic, and superconducting measurements. Unless otherwise noted, the T_s used below is assumed to be 400 °C. Cleaved single-crystal MgO(100) plates, glass plates, and thin polyimide films (7.5 μm) were used as substrates. The substrate dependence is discussed in Sec. III. A niobium layer was deposited on top to protect the Fe layers from oxidation. The covering Nb layer might show a surface superconductivity, giving us erroneous information. To check the possible occurrence of this surface effect, some samples with a thin covering Nb layer (3.0 nm) were examined. The samples with Nb layers thinner than 10.0 nm and Fe layers thicker than 1.0 nm did not become superconducting above 1.7 K. Thus the 3.0-nm Nb layer in contact with a thick Fe layer should be nonsuperconducting. If the surface effect affects the superconducting properties, some top-Nb-layer-thickness dependence should be observed. The measurements of T_c and H_{c2} showed no meaningful difference between them. Therefore, we conclude that the surface effect is negligible in this work.

III. STRUCTURAL PROPERTIES

The structural properties were investigated by an x-ray-diffraction (XRD) method. Both low- and high-angle XRD were measured using Cu $K\alpha$ radiation and a conventional θ -2 θ powder diffractometer. The samples composed of a few atomic Fe layers and thick Nb layers deposited on MgO substrates show bcc Nb(100) preferred orientation patterns in Fig. 1. The epitaxial growth of Nb(100)/MgO(100), Nb[011]/MgO[010] has been reported in spite of the large lattice mismatch (11%).⁷ Though there is no information about the in-plane structure in our case, the following experimental results suggest some epitaxial growth: the small full width at half maximum (FWHM) of the Nb(200) main peaks [(a) 0.3 and (b) 0.47] and a good coherence of the superstructure described below. Since the rocking curves of the main peaks broaden significantly, the crystal structure is not an ideal single crystal. Higher-order satellite peaks observed around Nb(200) [indicated by arrows in Figs. 1(a) and 1(b)] imply a good coherence in atomic-plane stacking with a well-regulated superstructure.

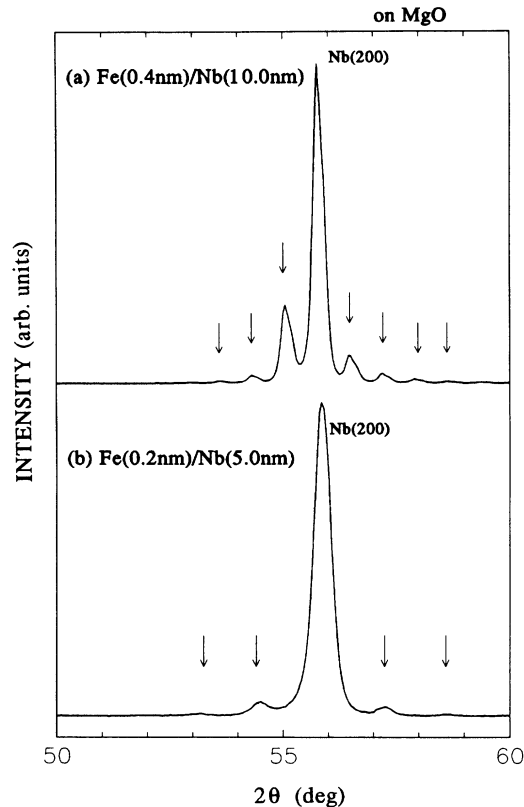


FIG. 1. High-angle x-ray diffraction of (a) $[\text{Fe}(0.4 \text{ nm})/\text{Nb}(10.0 \text{ nm})]_9$ and (b) $[\text{Fe}(0.2 \text{ nm})/\text{Nb}(5.0 \text{ nm})]_9$ multilayered films. Both films were deposited on single-crystal MgO(100) substrates. The substrate temperature was 200 °C. Satellite peaks around Nb(200) reflections are indicated by arrows.

A high- γ -ray-transmittance and small-susceptibility substrate is necessary for Mössbauer and magnetization measurements. A very thin (7.5 μm) polyimide film (UPILEX; produced by UBE-KOHSAN) satisfies these requirements. The UPILEX is also heat-stable up to 500 °C and mechanically tough. However, because it is not a single crystal, no epitaxial growth was expected. The prepared samples on this substrate were polycrystalline as shown in Fig. 2. Satellite peaks are generally not observed for polycrystalline multilayers; hence low-angle XRD measurements were performed to confirm the superstructure. Since sample misalignment is a serious problem in low-angle XRD work, such a flexible thin film is difficult to measure. A glass substrate is also noncrystalline and the film growth on it was expected to be similar to that on the UPILEX substrate. Clear superstructure reflections from first to third order are shown in Fig. 3. Thus, we are able to create well-regulated artificial superstructures on the noncrystalline substrates. Fine structures observed between the reflections are subsidiary maxima of the Laue function derived from a finite-size effect. The number of peaks between two reflections is equal to the number of bilayers. It means a good coherence of the superstructure throughout the whole sample. Most samples discussed in the following sections have

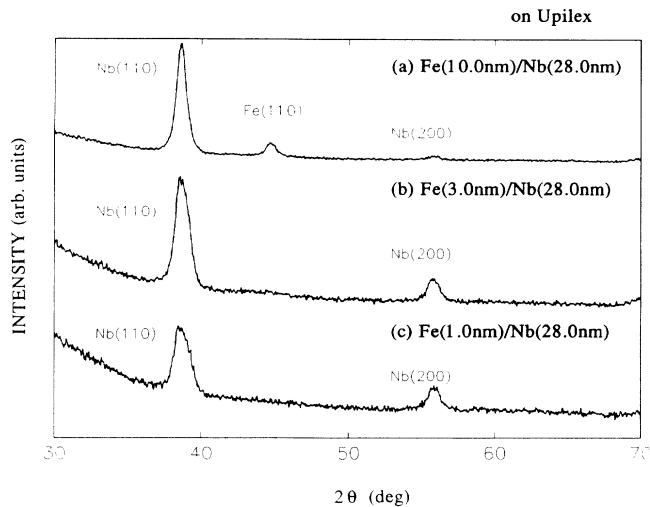


FIG. 2. High-angle x-ray diffraction of three multilayered films composed of different thickness Fe layers. These films were deposited on polyimide film (UPILEX) substrates.

large superstructure periodicities and the diffraction angles are too small to measure. It is generally believed that the preparation of multilayers with a large superstructure periodicity is easier than those with a smaller one. Therefore, we may conclude that results for samples with a small superstructure periodicity, such as those shown in Fig. 3, guarantee the successful formation of a larger superstructure periodicity.

IV. MAGNETIC PROPERTIES

The magnetic properties of samples on UPILEX substrate were investigated using the Mössbauer effect and SQUID susceptometry. The three magnetization curves in Fig. 4 were measured at 10 K. The samples are composed of thin Fe layers with different thicknesses and thick Nb layers. Figure 4(a) is considered to be a typical ferromagnetic magnetization curve. The magnetization saturates in a small field and a large remanent magnetization is observed. The 10.0-nm Fe layers are bcc Fe as

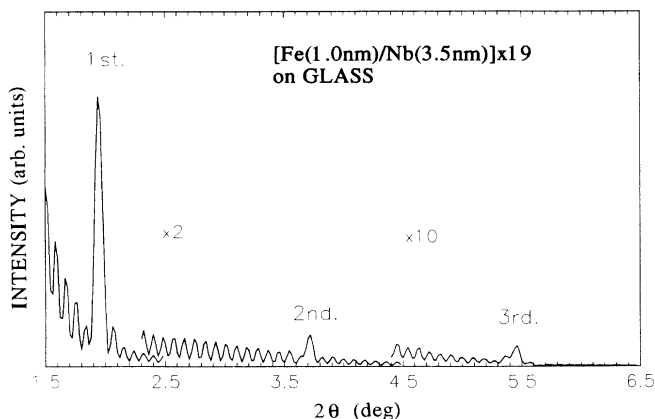


FIG. 3. A typical low-angle x-ray diffraction of a $[\text{Fe}(1.0\text{nm})/\text{Nb}(3.5\text{nm})]_{19}$ multilayered film.

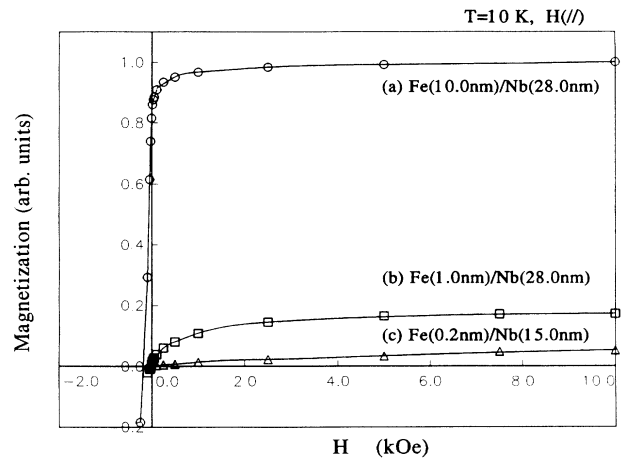


FIG. 4. Magnetization curves measured by SQUID. The measuring temperature was 10 K and the applied field was parallel to the film plane. The magnetization is normalized by the Fe-layer thickness.

shown in Fig. 2(a). These results are consistent with the Mössbauer spectrum in Fig. 5(a). A sharp splitting sextet absorption peak is seen in the spectrum at room temperature (RT). The hyperfine field calculated from the splitting is 330 kOe, which is nearly equal to the bulk Fe value. This means that long-range ferromagnetic ordering exists in the Fe layers and the magnetic moment has nearly the same magnitude as that of bulk Fe. No XRD reflection from the 3.0-nm Fe layers was observed as shown in Fig. 2(b). Both a paramagnetic (single peak) and a ferromagnetic (sextet bcc Fe) components exist in the Mössbauer spectrum of Fig. 5(b). The integrated intensity ratio is approximately 40:60 and the ferromagnetic component is still dominant. 3.0 nm seems to be a critical thickness at which Fe layers change from ferromagnetic to paramagnetic.

There is no significant structural difference between 3.0-nm [Fig. 2(b)] and 1.0-nm Fe [Fig. 2(c)] layers as judged from XRD measurements, while the difference in the magnetic properties is obvious. Only a paramagnetic single peak appears in the Mössbauer spectrum of Fig. 5(c) even at liquid-helium temperature (4.2 K). In the magnetization curve [Fig. 4(b)], the remanent magnetization seems to disappear. These results suggest paramagnetism in the 1.0-nm Fe layers. However, the curve in Fig. 4(b) shows saturation tendency in magnetization with a fairly small applied field. Moreover, the saturation magnetization is too large (about 20% of bulk Fe as shown in Fig. 4). This behavior can be explained by superparamagnetism, which usually appears in magnetically isolated particles but which is not expected to occur in these multilayered samples. Instead, we consider the following magnetic features of the 1.0-nm Fe layers. Small two-dimensional magnetic clusters of Fe atoms coupled with short-range ordering interact weakly with one another. The interaction is not strong enough to retain ferromagnetic long-range ordering against thermal fluctuation in zero field. The clusters become magnetically coupled with a small applied field. A similar fluctuat-

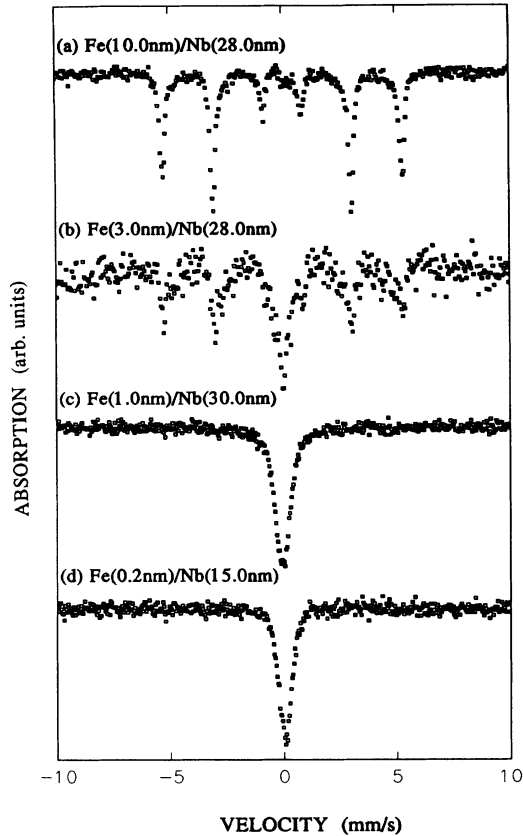


FIG. 5. Mössbauer absorption spectra. Spectra were measured at room temperature [(a) and (b)] and at liquid-helium temperature [(c) and (d)]. The Doppler shift velocity was calibrated using pure α -Fe.

ing magnetism has been reported in Fe/Mg multilayers.⁸

When the thickness of the magnetic layers decreases to a few atomic layers, magnetic ordering will become weak enough to be comparable to superconducting coherence. The Mössbauer spectrum [Fig. 5(d)] for the sample with monatomic Fe layers exhibits the same feature as Fig. 5(c). No hyperfine-field splitting implies no spontaneous magnetization, even at 4.2 K. The magnetization curve is somewhat different from that for the sample with 1.0-nm Fe layers. Curve (c) in Fig. 4 looks linear with no remanent magnetization. The temperature dependence of the susceptibility is Curie-like as shown in Fig. 6. These results indicate that the monatomic Fe layers are paramagnetic. It is not known whether the paramagnetism arises from alloying at the interfaces or from the two dimensionality. On the other hand, it is known that monatomic ferromagnetic layers sometimes show perpendicular anisotropy.⁸ In this case, however, such anisotropy was not observed as displayed in Fig. 7. An easy axis is in the film plane due to the shape anisotropy.

V. SUPERCONDUCTING PROPERTIES

The electrical resistances have been measured by use of a conventional four-terminal method. Since the measurement current densities were less than 2 A/cm², the self-heating effect was negligible and a superconducting tran-

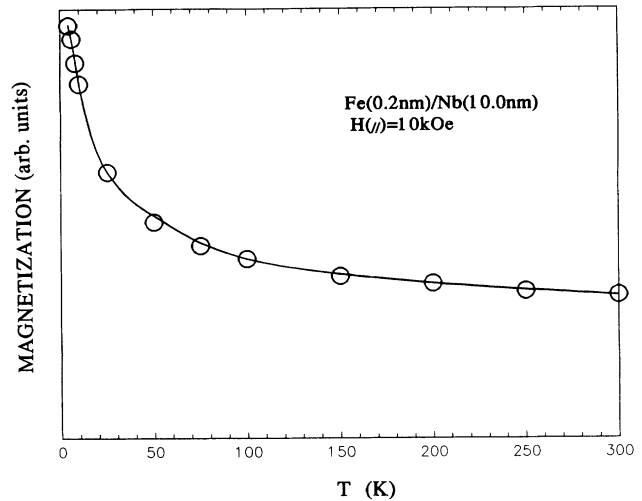


FIG. 6. Temperature dependence of the magnetization of an Fe(0.2 nm)/Nb(10.0 nm) multilayered film. A 10 kOe magnetic field was applied parallel to the film plane.

sition did not depend on the measurement current. Polyimide substrate samples were measured to compare the magnetic properties described above. The samples were cut into about 3×7 mm² rectangles. Four copper leads were connected with silver paste. Some MgO substrate samples were also measured to check the substrate dependence. There was no significant difference between them in superconducting transition temperatures (T_c). The superconducting magnet equipped with a 7-T split coil was employed to measure the upper critical fields (H_{c2}). The H_{c2} was defined as the applied field at a midpoint of the residual normal resistance. The applied field was swept at a constant temperature. The carbon glass resistance thermometer (Model CGR-1000, LakeShore Electronics) was used to measure the temperature under the field, because the resistance show little change under the applied

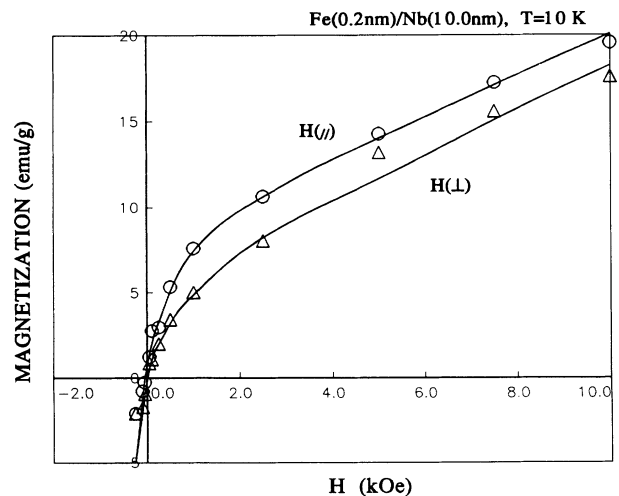


FIG. 7. Magnetization curves of a Fe(0.2 nm)/Nb(10.0 nm) multilayered film. Applied fields were parallel [$H(\parallel)$] and perpendicular [$H(\perp)$] to the film plane. The temperature measurement was 10 K.

field. The applied field was calculated from the coil current. The sample holder was wrapped with aluminum foil and put into the He exchange gas to reduce the temperature gradient. The measurement temperature was controlled by the heater mounted at the copper sample holder. A computer-controlled feedback system regulated the temperature deviation within 0.03 K during the measurement. The temperature ranged from 3.0 to 8.5 K. Both critical fields of parallel [$H_{c2\parallel}(T)$] and perpendicular [$H_{c2\perp}(T)$] to the film plane were measured.

The temperature dependence of the upper critical fields for four samples is displayed in Figs. 8 and 9. Figures 8(a) and 8(b) are results for the samples with ferromagnetic Fe layers. For these samples, $H_{c2\parallel}(T)$ is clearly larger than $H_{c2\perp}(T)$ throughout the temperature measurement range. The large anisotropy in the upper critical fields indicates the two-dimensional superconductivity. The large anisotropy was still observed for the sample with 1.0-nm Fe layers as shown in Fig. 9(a), although the Fe layers no longer exhibited spontaneous ferromagnetic ordering. When the Fe-layer thickness decreased further to the monatomic layer, the H_{c2} anisotropy displayed in Fig. 9(b) does not seem to be two dimensional. To clarify the dimensionality, we considered the characteristic features of the $H_{c2}(T)$. The temperature dependence of the upper critical fields may be expressed as follows:⁹

$$H_{c2\parallel}(T) = \frac{\phi_0}{2\pi} \frac{1}{\xi_{\parallel}(T)} \frac{1}{\xi_{\perp}(T)}, \quad (1)$$

$$H_{c2\perp}(T) = \frac{\phi_0}{2\pi} \frac{1}{\xi_{\parallel}^2(T)}, \quad (2)$$

where $\xi_{\parallel}(T)$ and $\xi_{\perp}(T)$ are the temperature-dependent coherence lengths, and ϕ_0 is the flux quantum. In the case of three-dimensional superconductivity, the $\xi_{\parallel}(T) \approx \xi_{\perp}(T)$ are proportional to $(1-t)^{-1/2}$ ($t = T/T_c$). Therefore, the relation between $H_{c2}(T)$ and reduced temperature t is written as

$$H_{c2\parallel}(T) \propto (1-t), \quad H_{c2\perp}(T) \propto (1-t). \quad (3)$$

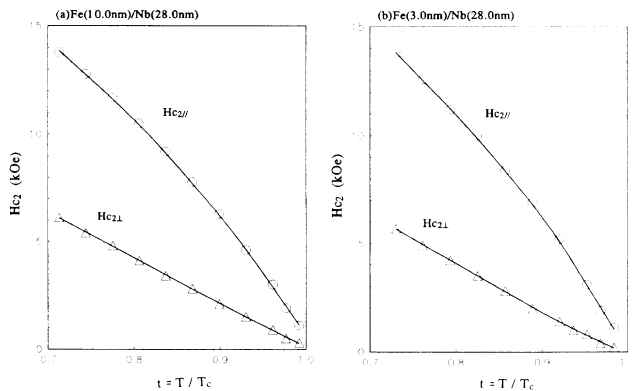


FIG. 8. Upper critical fields for the ferromagnetic samples as a function of the reduced temperature t ($\equiv T/T_c$). Applied fields were parallel $H_{c2\parallel}$ and perpendicular $H_{c2\perp}$ to the film plane.

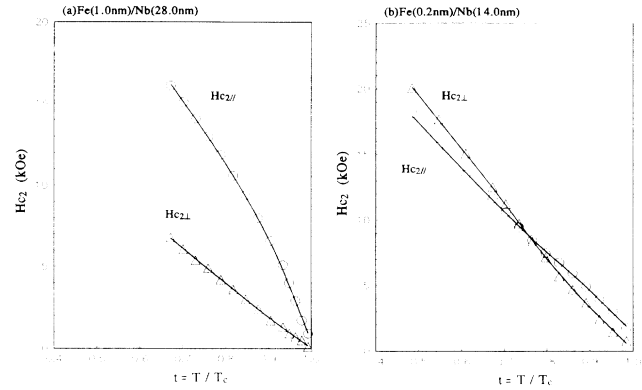


FIG. 9. Upper critical fields for the nonmagnetic samples as a function of the reduced temperature t ($\equiv T/T_c$). Applied fields were parallel $H_{c2\parallel}$ and perpendicular $H_{c2\perp}$ to the film plane.

That is, both $H_{c2\parallel}(T)$ and $H_{c2\perp}(T)$ are proportional to $(1-t)$, while the $\xi_{\perp}(T)$ is constant in the case of two-dimensional superconductivity. The constant value is considered to be an extent of superstructure period λ in this study. Therefore, the temperature dependence of the H_{c2} is expressed as

$$[H_{c2\parallel}(T)]^2 \propto (1-t), \quad H_{c2\perp}(T) \propto (1-t). \quad (4)$$

The $[H_{c2\parallel}(T)]^2$ is proportional to $(1-t)$. The squares of measured parallel upper critical fields, $[H_{c2\parallel}(T)]^2$ are plotted as a function of $(1-t)$ in Fig. 10 to examine the

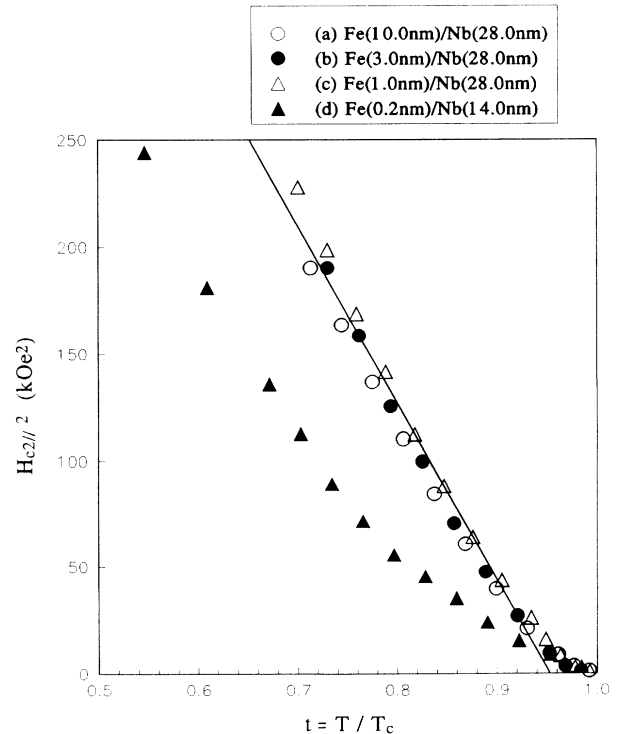


FIG. 10. Square of $H_{c2\parallel}$ vs the reduced temperature t ($\equiv T/T_c$).

dimensionality. The data of (a), (b), and (c) give a linear relationship except near T_c . The superconductivity is therefore two dimensional. On the other hand, data (d) show a parabolic behavior. It is therefore three dimensional, rather than two dimensional. The deviation of data (a)–(c) from the straight line near T_c is not understood. It is thought that $\xi_1(T)$ might penetrate into Fe layers to a certain extent.

Attention should be given to the anisotropy in Fig. 9(b). These H_{c2} curves cross around $T/T_c=0.75$. A similar crossover has been reported for the Ni/V system.⁴ In the Ni/V case, the $H_{c2\perp}(T)$ is larger than $H_{c2\parallel}(T)$ near T_c and the anisotropy is reversed at low temperature. One probable explanation proposed goes as follows:⁵ $\xi_1(T)$ is large enough near T_c and penetrates into the Ni layers. As a result, $H_{c2\parallel}(T)$ is strongly depressed by magnetic scattering in the Ni layers. $\xi_1(T)$ is confined within the V layers at low temperature. Since $H_{c2\parallel}(T)$ is nearly unaffected by the presence of Ni layers at this temperature, it exceeds $H_{c2\perp}(T)$. In our experiment, however, $H_{c2\parallel}(T)$ is larger near T_c and $H_{c2\perp}(T)$ exceeds it at low temperature. The anisotropy is reversed. Though this behavior is not fully understood, there is a possible explanation of the phenomenon. At first, we may neglect the surface effect as described in Sec. II. The monatomic Fe layers multilayering with thick Nb layers (10.0–15.0 nm) are paramagnetic as described in the previous section. Since the magnetic scattering effect is not strong enough to decouple the superconducting coherence, the behavior of $H_{c2}(T)$ is three dimensional throughout the temperature measurement range. In spite of the three dimensionality, the small anisotropy of $H_{c2}(T)$ may exist. Because the coherence length $\xi_{\parallel}(T)$, which depends on several material constants such as the density of states, diffusion constant, and conductivity,⁵ is generally anisotropic in layered samples, the interface pinning effect of the vortices also might contribute the anisotropy. Consequently, it is not unreasonable that $H_{c2\parallel}(T)$ exceeds $H_{c2\perp}(T)$ near T_c . Since $H_{c2}(T)$ increases with decreasing temperature, the induced magnetization under the ap-

plied critical field turns out to be large. The three-dimensional superconducting coherence is still maintained. The induced magnetization depresses the $H_{c2\parallel}(T)$ and the anisotropy reverts itself at low temperature. A similar result is obtained for another sample with Fe(0.2 nm)/Nb(10.0 nm). Samples composed of two atomic Fe layers or thin Nb layers (5.0 nm) did not show such unusual anisotropy. The behavior is considered to be very sensitive to the balance between ferromagnetism and superconductivity. These features, however, are not known in detail.

VI. SUMMARY

Multilayered films composed of a superconducting element (Nb) and a 3d ferromagnetic element (Fe) were prepared by an MBE method. Epitaxial growth is found to be possible on MgO single-crystal substrates. Well-regulated artificial superstructures are constructed on both single-crystal and noncrystalline substrates. For Fe-layer thickness less than 3.0 nm, the typical ferromagnetism disappeared. The samples composed of Fe layers thicker than 1.0 nm showed two-dimensional $H_{c2}(T)$ anisotropy. Fe layers are thought to destroy the superconducting interlayer coherence. When the thickness of Fe layers decreases to a monatomic layer, $H_{c2}(T)$ exhibits three-dimensional behavior. The ferromagnetic ordering in the Fe layers does not determine the superconducting dimensionality of the multilayered films. This conclusion is different from that obtained for the Ni/V system.⁴ Some samples consist of monatomic Fe layers and showed unusual $H_{c2}(T)$ anisotropy. The behavior is considered to be related to the paramagnetic properties of the monatomic Fe layers.

ACKNOWLEDGMENTS

The authors would like to thank K. Nomura and E. Akiba for help in XRD measurements, and B. Engel, Y. Oosawa, and K. Fukuda for fruitful discussions.

¹O. Fisher, in *Ferromagnetic Materials*, edited by K. H. J. Buschow and E. P. Wohlfarth (North-Holland, Amsterdam, 1990), Vol. 5, p. 465.

²T. Claeson, *Thin Solid Films* **66**, 151 (1980).

³H. K. Wong, B. Y. Jin, H. Q. Yang, J. B. Ketterson, and J. E. Hilliard, *J. Low Temp. Phys.* **63**, 307 (1986).

⁴H. Homma, C. S. L. Chun, G. G. Zheng, and I. K. Shuller, *Phys. Rev. B* **33**, 3562 (1986).

⁵S. Takahashi and M. Tachiki, *Phys. Rev. B* **33**, 4620 (1986).

⁶C. M. Falco and I. K. Schuller, in *Synthetic Modulated Structures*, edited by L. L. Chang and B. C. Giessen (Academic, New York, 1985), p. 340.

⁷G. Oya, M. Koishi, and Y. Sawada, *J. Appl. Phys.* **60**, 1440 (1986).

⁸K. Kawaguchi, R. Yamamoto, N. Hosoito, T. Shinjo, and T. Takada, *J. Phys. Soc. Jpn.* **55**, 2375 (1986).

⁹C. Uher, J. L. Cohn, and I. K. Shuller, *Phys. Rev. B* **34**, 4906 (1986).